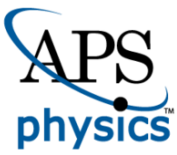

Inverse Spin Hall Effect in a Ferromagnetic Metal

B. F. Miao, S. Y. Huang, D. Qu, and C. L. Chien

Phys. Rev. Lett. **111**, 066602 — Published 5 August 2013

DOI: 10.1103/PhysRevLett.111.066602

Inverse Spin Hall Effect in a Ferromagnetic Metal

B. F. Miao[1,2], S. Y. Huang[1], D. Qu[1], and C. L. Chien[1*]

[1] Department of Physics and Astronomy, Johns Hopkins University, Baltimore, MD 21218, USA

[2] National Laboratory of Solid State Microstructures and Department of Physics, Nanjing University, Nanjing 210093, China

Abstract:

Inverse spin Hall effect (ISHE) has been observed only in non-magnetic metals, such as Pt and Au, with a strong spin-orbit coupling. We report the observation of ISHE in a ferromagnetic permalloy (Py) on ferromagnetic insulator yttrium iron garnet (YIG). Through controlling the spin current injection by altering the Py/YIG interface, we have isolated the spin current contribution and demonstrated the ISHE in a ferromagnetic metal, the reciprocal phenomenon of anomalous Hall effect. A large spin Hall angle in Py, determined from Py thin films of different thicknesses, indicates many other ferromagnetic metals may be exploited as superior pure spin current detectors and for applications in spin current.

PACS numbers: 72.15.Jf , 72.20.Pa, 72.25.-b, 85.80.-b

Recently, a great deal of attention has been focused on pure spin current, its generation, detection, and exploitation. In contrast to a spin-polarized current, a pure spin current has the unique attribute of using a minimal charge carriers to deliver substantial angular momentum thus generating much less Joule heat. However, a pure spin current cannot be generated by the usual electrical means except through a few mechanisms, among them spin Hall effect (SHE) [1-3], lateral spin valve [4, 5], spin pumping [6-8] and spin Seebeck effect (SSE) [9, 10], by exploiting heavy (high-Z) metals with strong spin-orbit coupling (SOC) for the generation/detection of the pure spin current. When a charge current passes through a metal with strong SOC, the SHE causes electrons with opposite spin to drift in opposite direction thus generating a transverse pure spin current [Fig. 1(a)] with a density of $\vec{J}_S = \theta_{SH} \frac{\hbar}{2e} \vec{J}_C \times \vec{\sigma}$, where θ_{SH} is the spin Hall angle, $\vec{\sigma}$ the spin direction, $\hbar$ is the reduced Planck constant and e is the electronic charge. A pure spin current cannot be detected electrically but by the inverse spin Hall effect (ISHE) again in a strong SOC metal that converts it into a charge current of density $\vec{J}_C = \theta_{SH} \frac{2e}{\hbar} \vec{J}_S \times \vec{\sigma}$ in the transverse direction, resulting in charge accumulation at the sample edges [Fig. 1(b)].

In a ferromagnetic metal, the electrons are polarized with unequal number of electrons with opposite spin. When a charge current of density J_C flows in a ferromagnetic metal, the anomalous Hall effect (AHE) compels electrons of opposite spin to drift in opposite direction, thus creating a spin polarized current of density J_{SP} in the transverse direction, as shown in Fig. 1(c) [11]. The interesting scenario is when a pure spin current is injected into a ferromagnetic metal as shown in Fig. 1(d). Similar to the

situation of ISHE in a non-magnetic metal [Fig. 1(b)], one may expect ISHE in a ferromagnetic metal to likewise generate a transverse charge current and charge accumulation. However, demonstration of ISHE in a ferromagnetic metal is far more challenging because of the presence of the charge current and other effects associated with the ferromagnetic metals.

In this work, we report the observation of ISHE in a ferromagnetic metal of permalloy (Py) by separating out phenomena of spin current from those of charge current. The ISHE in ferromagnetic metals is the inverse effect of the anomalous Hall effect (AHE). Using Py of various thicknesses, we have determined θ_{SH} for Py with a value comparable to that of Pt. The realization of ISHE in ferromagnetic metals greatly expands the varieties of materials that can be exploited for spin current phenomena, including the use of inexpensive materials with exceptionally larger spin Hall angle.

Experimentally, we use longitudinal SSE with a well-defined out-of-plane temperature gradient $\nabla_z T$ to inject a pure spin current from yttrium iron garnet (YIG) into either a non-magnetic metal (Pt) or a ferromagnetic (Py) thin film [12, 13]. Intrinsic SSE has recently been reported using the longitudinal spin current injection that has eluded detection in the transverse configuration using thin film on thick substrate [14, 15]. Under an out-of-plane $\nabla_z T$, only spin current phenomena are realized in Pt/YIG, whereas in Py/YIG, in addition to spin current effects, there is also the anomalous Nernst effect (ANE) inherent to Py [16]. However, the pure spin current phenomena require a spin current injected *across* the interface between metal and YIG. Thus in Pt/YIG and Py/YIG all spin current phenomena would necessarily cease if one intentionally blocks the

transmission of the spin current. We demonstrate in Pt/YIG that altering the YIG surface before the metal deposition, or more decisively, by inserting an insulating layer between YIG and the metal layer, can accomplish this feat. In Py/YIG, signals from both ISHE and ANE are present, whereas after the interface has been altered, only that of ANE remains. The difference between the two provides a direct measurement of the ISHE in Py.

We have deposited Pt(t) and Py(t) thin films of various thicknesses t by magnetron sputtering onto polycrystalline YIG substrates (typically 6 mm x 3 mm x 0.5 mm) and patterned the thin films into a Hall bar structure consisting of one long (5 mm) segment of width 0.2 mm with three short side-bars 1.5 mm apart as shown in Fig. 2(a). Four-terminal method has been used to measure magnetoresistance with current along the long segment (I_{12}) and voltage from the two side-bars (V_{34}). We denote the xyz-axes as those parallel to the YIG substrate edges with the x-axis along the long segment. Magnetic field $\boldsymbol{H}$ (1.5 T) is rotated within the xy, xz, and yz planes to obtain the angular dependences of the magnetoresistance on ϕ_{xy}, α_{xz} and θ_{yz} respectively as shown in Fig. 2(a). For the thermal measurements, the thermal voltage V_{th} has been measured at V_{12} under a uniform temperature gradient ($\nabla_z T$) with a temperature difference of 10 K under a magnetic field applied at ϕ_{xy} with respect to the x-direction in the sample plane.

For Pt/YIG, in the longitudinal SSE under $\nabla_z T$, the spin current from YIG gives rise to the voltage V_{th} detected within the Pt layer via the ISHE of $E_{ISHE} \propto \vec{J}_S \times \vec{\sigma}$. Rotating H at ϕ_{xy} in the sample plane, one obtains $E_{ISHE} \propto \sin\phi_{xy}$. The thermal voltage V_{th} reaches the maximum value when H is along the $\pm y$-axis ($\phi_{xy} = \pm 90°$). In Figure 2. (b), the

black curve shows the field dependent thermal voltage V_{th} for Pt(3 nm)/YIG, when the H is along the y-axis (ϕ_{xy} =90°). The thermal voltage V_{th}, with a magnitude of 9.9μV, is asymmetric in H and with a field dependence following that of the YIG's magnetization curve. The hysteretic behavior in Fig. 2 (b) is the signature from the magnetic grains of polycrystalline YIG [16].

In other Pt/YIG samples, prior to the Pt deposition, we have used Ar ion beam bombardment (500 V, current density 0.4 mA/cm^2) on the YIG substrate for 5 minutes to alter the surface, or depositing a 5-nm MgO layer on YIG. These samples are labeled as Pt(t)/YIG$_{BB}$, where the subscript BB denotes 5 min of ion bombardment, and Pt(t)/MgO(5 nm)/YIG respectively. Most significantly, while a large V_{th} exists in Pt(3 nm)/YIG, there is *no* measureable spin dependent thermal voltage in Pt(3 nm)/YIG$_{BB}$ and Py(3 nm)/MgO(5 nm)/YIG, shown as the red and blue horizontal lines in Fig. 2(b) respectively. Thus, altering the YIG surface by either ion bombardment or by inserting a MgO(5 nm) layer can *completely* block spin current injection across the metal/YIG interface. This crucial aspect will be exploited in extracting ISHE in Py. It also underscores the importance of surface quality between metal and YIG for spin current injection.

Before further discussion, we mention the new magnetoresistance (MR) phenomena recently observed in Pt/YIG [13, 16-18]. Figure 2(c) shows the MR behavior of Pt(3 nm)/YIG. The MR ratio of $(R_{\parallel} - R_T)/R_T$ is about 2.2×10^{-4}, where $R_{\parallel}(\phi_{xy} = 0°)$ and R_T ($\phi_{xy} = 90°$) are the longitudinal and transverse MR respectively. The MR behavior with an in-plane field is identical to the well-known anisotropic MR (AMR) in ferromagnetic

metals with $R(\phi_{xy}) = R_T + (R_{\parallel} - R_T)\cos^2\phi_{xy}$ [19, 20]. In conventional AMR, resistance is determined by the angle between magnetization $\boldsymbol{M}$ and the current direction, thus, $R_{\parallel} > R_T \approx R_{\perp}$, where $R_{\perp}$ is the perpendicular MR. In contrast, Pt/YIG exhibits a totally different behavior of $R_{\perp} \approx R_{\parallel} > R_T$. The mechanism of the new MR remains to be identified, although spin Hall MR [18] and magnetic proximity MR [17] have been proposed.

Under argon ion etching, as a result of the different sputtering yields of Y, Fe, and O[21-23], the surface composition is altered from that of bulk YIG, but the remnant iron atoms remain. Interestingly, this new MR is *preserved* in Pt(3 nm)/YIG_{BB} [Fig. 2(d)] showing the same angular dependence and similar magnitude as that of Pt/YIG [Fig. 2(c)], while the spin-dependent thermal voltage V_{th} completely disappears. This suggests that the new MR at high field is unlikely to be related to spin current. We attribute it to the proximity effect with the iron atoms on the YIG surface. In the case of Pt(3 nm)/MgO(5 nm)/YIG, it shows no MR nor thermal voltage; the resistance is independent of field or field direction, same as that of Pt(3 nm)/Si.

We next discuss Py/YIG, the system of interest. Since Py is ferromagnetic, under the same $\nabla_z T$, in addition to the injection of spin current, which gives rise to ISHE, there is also the ANE within ferromagnetic Py of $E_{ANE} \propto \nabla_Z T \times \vec{m}$, where $\vec{m}$ denote the direction of magnetization [Fig. 3(a)]. In the longitudinal SSE configuration, because $\nabla_Z T \parallel \vec{J}_S$ and $\vec{m} \parallel \vec{\sigma}$, ISHE and ANE are additive[16]. However, the Pt/YIG results indicate that the altered YIG surface by ion bombardment or by the insertion of a MgO layer can terminate the flow of spin current [Fig. 3(b)]. This allows us to separate the ISHE from

the ANE. As shown in Fig. 3(c), the Py(5 nm)/YIG sample exhibits a thermal voltage V_{th} with a magnitude of 4.2 μV, which consists of the ANE signal within Py and the ISHE signal due to the pure spin current injected from YIG. In Py(5 nm)/YIG_{BB} and Py(5 nm)/MgO(5 nm)/YIG, exhibiting the same results, there is no spin current into the Py layer, and only the ANE in Py remains. As a result, the maximal thermal voltage decreases substantially from 4.2 μV to 0.9 μV. The large difference of V_{th} between the unaltered interface in Py(5 nm)/YIG and the altered interface in Py(5 nm)/YIG_{BB} and Py(3 nm)/MgO(5 nm)/YIG is V_{ISHE}, the result of the *inverse spin Hall effect* in the ferromagnetic Py. Figure 3(d) shows the angular dependence of V_{th} for Py(5 nm)/YIG and Py(5 nm)/YIG_{BB} respectively. Both curves follow the $\sin\phi$ behavior, confirming that ANE and ISHE share the same angular dependence and V_{ISHE} is the difference between the two curves.

The thermal injection of spin current in longitudinal geometry offers the advantages of using a very thin spin current detector layer with a thickness comparable to, or even less than, the spin diffusion length λ_{sf}. However, it is essential to measure a series of Py with different thickness to obtain the values of θ_{SH} and the λ_{sf}. By subtracting intrinsic ANE of Py from thermal voltage, we obtain V_{ISHE} in each case. Figure 4(a) and (b) displays the dependence of resistivity ρ and thermal voltage V_{ISHE} on Py thickness. While at large thicknesses ρ is a constant, at small thickness ρ increases with decreasing film thickness due to surface scattering, in a manner well described by the Fuchs-Sondheimer therory [24]. Within the same thickness range of 30 nm, V_{ISHE} also increases with decreasing film thickness. The magnitude of ISHE is proportional to θ_{SH} as well as ρ

in the spin current detector. Thus, quantitative analysis of θ_{SH} requires the knowledge of the thickness and the resistivity of the spin current detector. As shown in Fig. 4(b), when the spin current detector is too thick, there is no V_{ISHE} to be realized.

For the same thickness of 3 nm, the values V_{ISHE} and ρ for Py and Pt are comparable, suggesting similar values of θ_{SH}. However, a quantitative determination requires a series of samples fabricated and measured under very similar conditions. As in all pure spin current phenomena, the main uncertainty is the spin current injection efficiency across the interface. While one can drastically reduce its efficiency, one does not know the transparency of the interface before alteration. We assume that before alteration, the spin current injection efficiency remains the same among our sample, represented by a pure spin current injection coefficient C, where $\frac{2e}{\hbar}\vec{J}_S(0) = C\nabla T$, $\vec{J}_S(0)$ is the spin current density at the interface and ∇T is the temperature gradient. After injection, the spin current decays as it travels along the z direction into the metal according to

$$\vec{J}_S(z) = \vec{J}_S(0)\frac{\sinh[(t_{Py} - z)/\lambda_{sf}]}{\sinh(t_{Py}/\lambda_{sf})}, \quad (1)$$

where λ_{sf} and t_{Py} are the spin diffusion length and the thickness of Py [8, 25]. The pure spin current gives rise to a transverse charge current via the ISHE, $\vec{J}_C(z) = \theta_{SH}\frac{2e}{\hbar}\vec{J}_S(z)\times\vec{\sigma}$, with $\vec{\sigma}$ pointing along the y-axis. Thus, the thermal voltage from ISHE in Py can be obtained from

$$V_{ISHE} = \frac{\rho L}{t_{Py} W} \int \left(\vec{J}_C \bullet \vec{x} \right) ds = C \nabla T \theta_{SH} \lambda_{sf} \frac{\rho L}{t_{Py}} \tanh\left(\frac{t_{Py}}{2\lambda_{sf}} \right), \quad (2)$$

$$V_{ISHE} / \rho \propto \theta_{SH} \frac{\lambda_{sf}}{t_{Py}} \tanh\left(\frac{t_{Py}}{2\lambda_{sf}} \right), \quad (3)$$

where $L \approx 4.2$ mm and $W = 0.2$ mm are the length and width of the Py film respectively in our measurements. The decay characteristics of V_{ISHE} and ρ for very thin layers are different as dictated by λ_{sf} and the carrier mean free path respectively, underscoring the importance of obtaining the thickness dependence of both V_{ISHE} and ρ in order the extract the value of θ_{SH}. The insert in Figure 4(b) shows the thickness dependence of V_{ISHE}/ρ. Fitting the experimental data with Eq.(3) yields λ_{sf} =2.5 nm, which is consistent with those reported for Py [26, 27]. This indicates that the spin current is mainly carried by the conduction electrons. On the other hand, the determination of θ_{SH}(Py) requires the absolute value of C, the injection efficiency at the interface. Assuming similar injection efficient for Py/YIG as those of other *5d* metals (e.g. Pt) on YIG [28], we have θ_{SH}(Py)/θ_{SH}(Pt)≈0.38. By using θ_{SH}(Pt)=0.014 [28], we obtain θ_{SH}(Pt)=0.005. These results show Py has a comparably large spin Hall angle as Pt and thus with similar V_{ISHE} values. More importantly, this observation paves the way to exploit many other ferromagnetic metals as superior pure spin current detectors for exploring pure spin current effects and applications.

In summary, we have observed inverse spin Hall effect in permalloy due to spin current injected from YIG via a thermal gradient. Altering the YIG surface by ion etching

or inserting an insulating layer can completely block the passage of the spin current, thus allowing us to extract quantitatively the contributions of the pure spin current from other charge current effects. We find that the new MR at high field observed in Pt/YIG has no direct correlation with the spin current from YIG. Through the measurements of samples with different thicknesses we have determined a sizable spin Hall angle of permalloy. Equally significant, one can now incorporate a vast number of ferromagnetic materials with different attributes in the exploration of pure spin current phenomena.

Acknowledgements

This work was supported by DOE (DE-SC0009390). B.F.M. was supported by the Yeung Center at JHU and the State Key Program for Basic Research of China (Grant No. 2010CB923401). S.Y.H. was partially supported by STARnet, a SRC program sponsored by MARCO and DARPA.

References:

* C. L. Chien (clc@pha.jhu.edu)

[1] J. E. Hirsch, Phys. Rev. Lett. **83**, 1834 (1999).
[2] Y. K. Kato, R. C. Myers, A. C. Gossard, and D. D. Awschalom, Science **306**, 1910 (2004).
[3] M. I. Dyakonov and V. I. Perel, Phys. Lett. A **35**, 459 (1971).
[4] S. O. Valenzuela and M. Tinkham, Nature **442**, 176 (2006).
[5] T. Kimura, Y. Otani, T. Sato, S. Takahashi, and S. Maekawa, Phys. Rev. Lett. **98**, 156601 (2007).
[6] E. Saitoh, M. Ueda, H. Miyajima, and G. Tatara, Appl. Phys. Lett. **88**, 182509 (2006).
[7] K. Ando, Y. Kajiwara, S. Takahashi, S. Maekawa, K. Takemoto, M. Takatsu, and E. Saitoh, Phys. Rev. B **78**, 014413 (2008).
[8] O. Mosendz, J. E. Pearson, F. Y. Fradin, G. E. W. Bauer, S. D. Bader, and A. Hoffmann, Phys. Rev. Lett. **104**, 046601 (2010).

[9] K. Uchida, S. Takahashi, K. Harii, J. Ieda, W. Koshibae, K. Ando, S. Maekawa, and E. Saitoh, Nature **455**, 778 (2008).
[10] K. Uchida, *et al.,* Nature Mater **9**, 894 (2010).
[11] E. H. Hall, Philos. Mag. **19**, 301 (1880).
[12] K.-i. Uchida, H. Adachi, T. Ota, H. Nakayama, S. Maekawa, and E. Saitoh, Appl. Phys. Lett. **97**, 172505 (2010).
[13] M. Weiler, *et al.,* Phys. Rev. Lett. **108**, 106602 (2012).
[14] S. Y. Huang, W. G. Wang, S. F. Lee, J. Kwo, and C. L. Chien, Phys. Rev. Lett. **107**, 216604 (2011).
[15] D. Qu, S. Y. Huang, J. Hu, R. Wu, and C. L. Chien, Phys. Rev. Lett. **110**, 067206 (2013).
[16] S. Y. Huang, X. Fan, D. Qu, Y. P. Chen, W. G. Wang, J. Wu, T. Y. Chen, J. Q. Xiao, and C. L. Chien, Phys. Rev. Lett. **109**, 107204 (2012).
[17] Y. M. Lu *et al.* to be published.
[18] H. Nakayama, *et al.,* Phys. Rev. Lett. **110**, 206601 (2013).
[19] T. R. McGuire and R. I. Potter, IEEE Trans. Magn. **11**, 1018 (1975).
[20] R. C. O'handley, *Modern magnetic materials: principles and applications* (Wiley New York, 2000).
[21] N. Matsunami, Y. Yamamura, Y. Itikawa, N. Itoh, Y. Kazumata, S. Miyagawa, K. Morita, R. Shimizu, and H. Tawara, At. Data. Nucl. Data Tables **31**, 1 (1984).
[22] J. E. Mahan and A. Vantomme, Phys. Rev. B **61**, 8516 (2000).
[23] M. P. Seah, Nucl. Instr. Meth. B **229**, 348 (2005).
[24] P. Fan, K. Yi, J.-D. Shao, and Z.-X. Fan, J. Appl. Phys. **95**, 2527 (2004).
[25] Z. Feng, *et al.,* Phys. Rev. B **85**, 214423 (2012).
[26] T. Kimura, J. Hamrle, and Y. Otani, Phys. Rev. B **72**, 014461 (2005).
[27] S. Dubois, L. Piraux, J. M. George, K. Ounadjela, J. L. Duvail, and A. Fert, Phys. Rev. B **60**, 477 (1999).
[28] D. Qu *et al.* to be published.

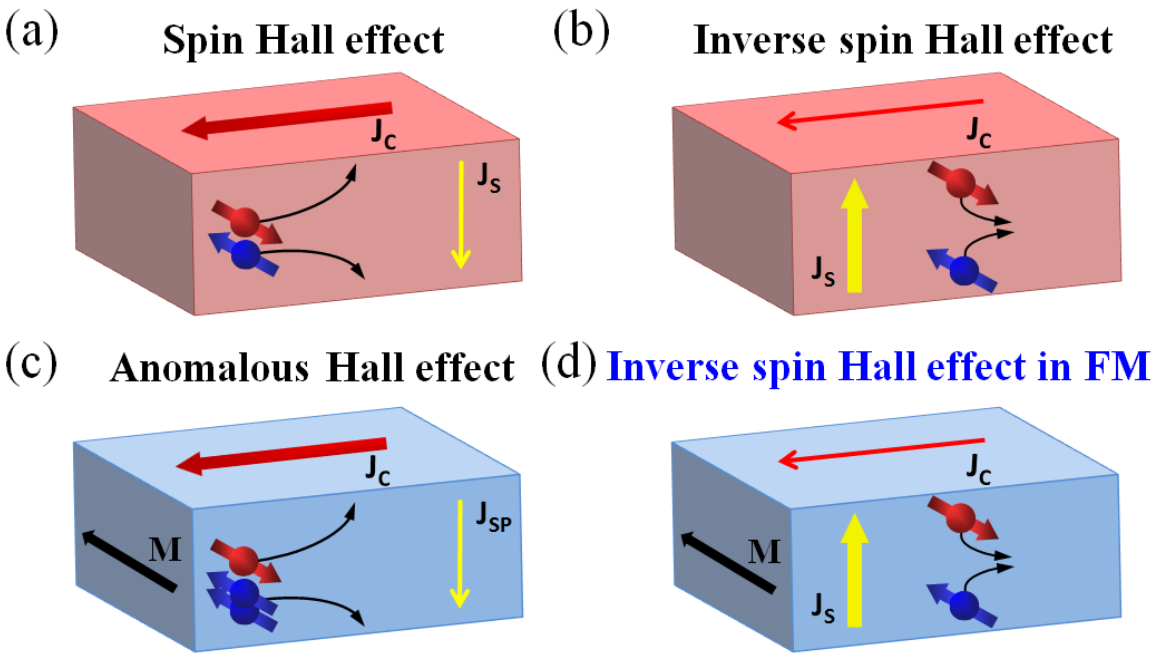

Fig. 1 (color online). Schematic diagrams of (a) spin Hall effect, (b) inverse spin Hall effect in a non-magnetic metal as well as (c) anomalous Hall effect, (d) inverse spin Hall effect in a ferromagnetic metal, illustrating the generation of charge current ($\boldsymbol{J_c}$), spin current ($\boldsymbol{J_S}$) and spin-polarized current ($\boldsymbol{J_{SP}}$) from the transport of spin-up and spin-down electrons.

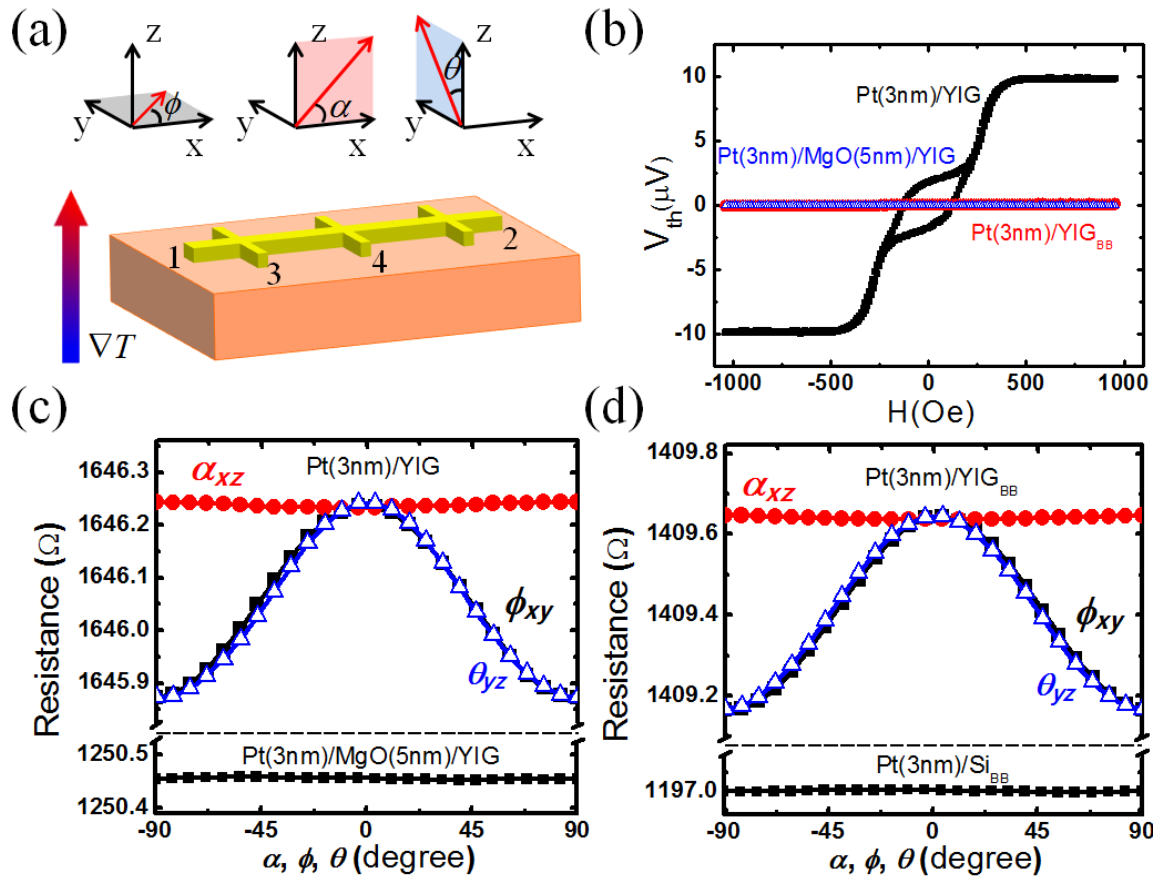

Fig. 2 (color online). (a) Schematics of the patterned Hall-bar sample with labeled terminals on a YIG substrate with edges parallel to the *xyz* axes and thermal gradient along the *z*-axis. (b) Field dependence of thermal voltage V_{th} for Pt(3 nm)/YIG, Pt(3 nm)/MgO(5 nm)/YIG, and Pt(3 nm)/YIG$_{BB}$ after ion bombardment for 5 min on YIG. Angular dependence of MR of (c) Pt(3 nm)/YIG and (d) Pt(3 nm)/YIG$_{BB}$ in the ϕ_{xy}(black), α_{xz}(red), and θ_{yz} (blue) scans where the magnetic field has been applied in the *xy, xz,* and *yz* planes at angles ϕ, α, and θ with the coordinate axes as shown in (a). The lower panels in (c) and (d) show the null MR results for Pt(3 nm)/MgO(5nm)/YIG and Pt(3 nm)/Si$_{BB}$ respectively.

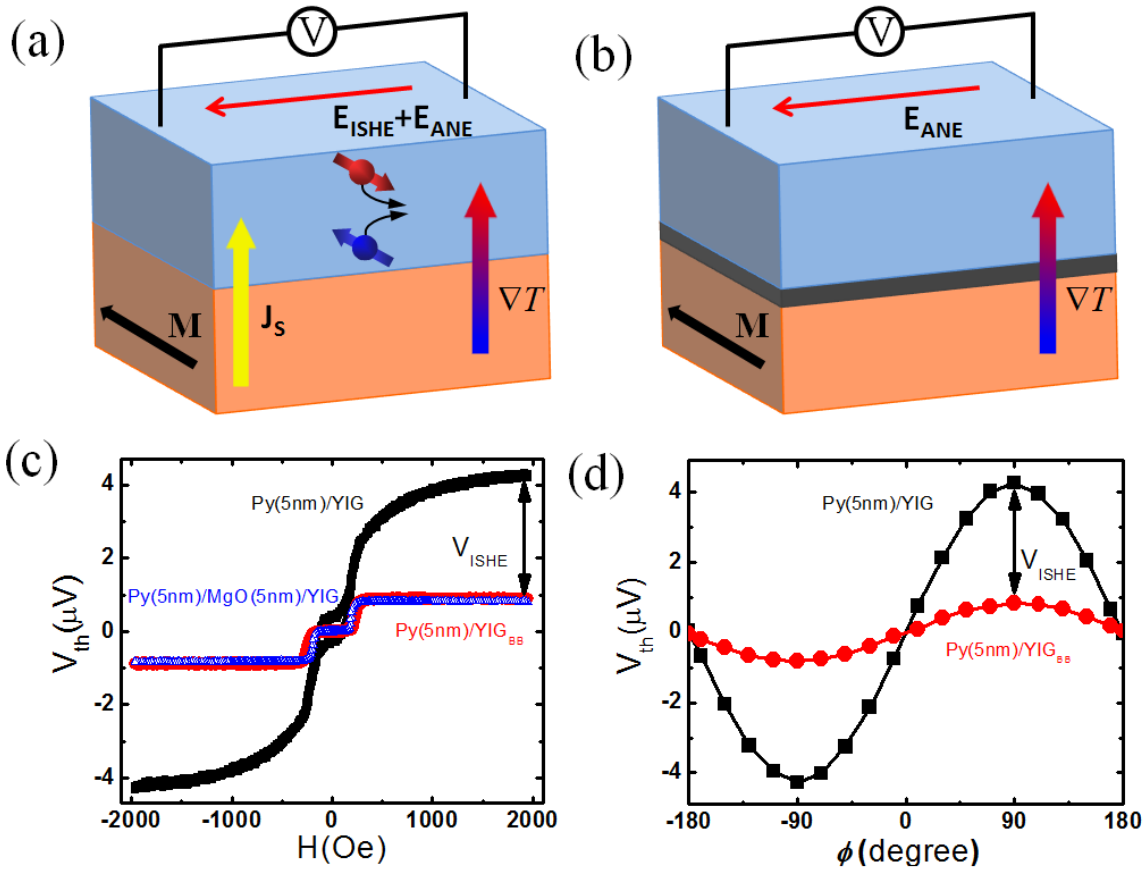

Fig. 3 (color online). Schematic diagrams for (a) Py/YIG and (b) Py on alterd YIG under perpendicular temperature gradient. (c) Field dependence of thermal voltage V_{th} for Py(5 nm)/YIG (black), Py(5 nm)/MgO(5 nm)/YIG (blue), and Py(5 nm)/YIG_{BB} (red) after ion bombardment for 5 min on YIG. The voltage difference V_{ISHE} gives the contribution exclusive to the inverse spin Hall effect in Py. (d) Angular dependence of thermal voltage V_{th} for Pt(5 nm)/YIG (black), and Py(5 nm)/YIG_{BB} (red).

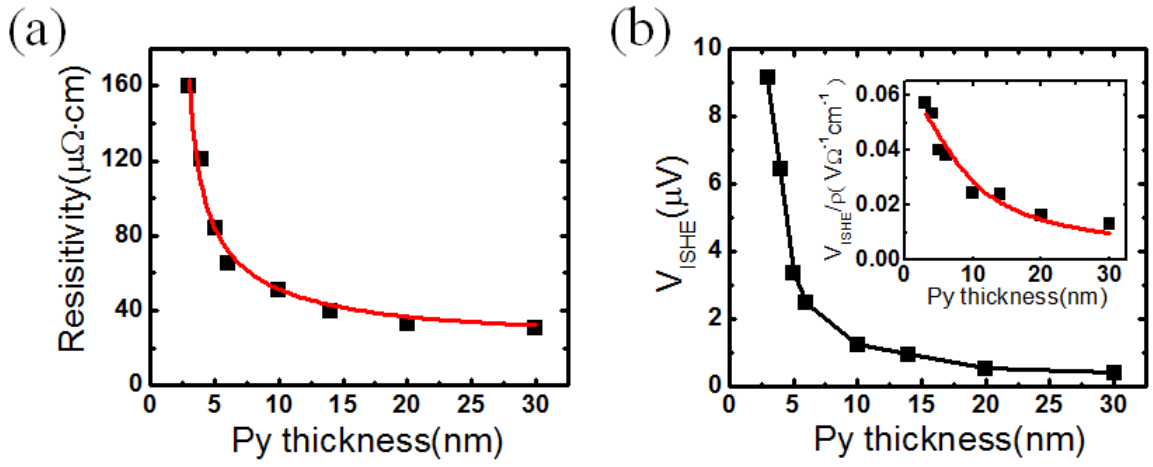

Fig. 4 (color online). (a) Thickness dependence of resistivity ρ for Py/YIG; the red curve is from the Fuchs-Sondheimer therory. (b) Thickness dependence of V_{ISHE} of Py/YIG. The insert shows the thickness dependence of V_{ISHE}/ρ, where the red curve is the best-fit result using equation (3).